

## INVESTIGATIONS OF CRYSTAL-CHEMICAL VARIABILITY IN LEAD URANYL OXIDE HYDRATES. II. FOURMARIERITE

YAPING LI AND PETER C. BURNS<sup>§</sup>

*Department of Civil Engineering and Geological Sciences, University of Notre Dame, 156 Fitzpatrick Hall,  
Notre Dame, Indiana 46556-0767, U.S.A.*

### ABSTRACT

Structures have been refined for twelve crystals of fourmarierite from various localities in the Democratic Republic of Congo, and one synthetic crystal. Single-crystal diffraction data were collected using MoK $\alpha$  X-radiation and a CCD-based detector mounted on a Bruker three-circle diffractometer. All crystals have orthorhombic symmetry, space group  $Bb2_1m$ . The natural crystals have similar unit-cell parameters:  $a$  14.00–14.03,  $b$  16.40–16.48,  $c$  14.32–14.38 Å. The parameters for the synthetic crystal, which contains less Pb than the natural crystals, are  $a$  13.938(2),  $b$  16.638(3),  $c$  14.672(2) Å. The structures refined to agreement indices ( $R1$ ) in the range of 3.6 to 6.2%. The structure of fourmarierite contains uranyl pentagonal bipyramids that share edges and corners to form sheets oriented parallel to (001). There are two distinct Pb<sup>2+</sup> cations and eight H<sub>2</sub>O groups located in the interlayer. On the basis of the structure refinements, the site occupancy of Pb(1) in the natural crystals is typically deficient, ranging from 71 to 100%, whereas the site occupancy of Pb(2) is ~100% in the crystals studied. In the synthetic crystal the Pb(1) and Pb(2) occupancies are 13% and 87%, respectively. Increase of the Pb content is correlated with a minor increase in the  $a$  unit-cell parameter, as well as large decreases in the  $b$  and  $c$  unit-cell parameters, and the unit-cell volume. The substitution  $O^{2-} \leftrightarrow (OH)^-$  at two anion sites [O(12) and O(15)] in the sheet of uranyl polyhedra provides the charge-balance mechanism associated with interlayer cation variation. The structural formula for fourmarierite may be written as  $Pb_{1-x}[(UO_2)_4O_{3-2x}(OH)_{4+2x}](H_2O)_4$ ,  $Z = 8$ , with the constituents of the sheet of uranyl polyhedra enclosed in square braces.

*Keywords:* fourmarierite, uranyl mineral, structure determination, crystal chemistry.

### SOMMAIRE

Nous avons affiné la structure de douze cristaux de fourmariérite provenant de diverses localités de la République Démocratique du Congo, et d'un cristal synthétique. Les données ont été prélevées sur cristal unique avec rayonnement MoK $\alpha$  et un diffractomètre à trois cercles Bruker muni d'un détecteur de type CCD. Tous les cristaux possèdent une symétrie orthorhombique, groupe spatial  $Bb2_1m$ . Les cristaux naturels ont des paramètres réticulaires semblables:  $a$  14.00–14.03,  $b$  16.40–16.48,  $c$  14.32–14.38 Å. Les paramètres du cristal synthétique, qui contient moins de Pb que les cristaux naturels, sont  $a$  13.938(2),  $b$  16.638(3),  $c$  14.672(2) Å. Les structures ont été affinées jusqu'à un résidu  $R1$  entre 3.6 et 6.2%. La structure de la fourmariérite contient des bipyramides à uranyle pentagonales qui partagent arêtes et coins pour former des feuillettes parallèles à (001). Il y a deux sites distincts occupés par des cations Pb<sup>2+</sup> et huit groupes H<sub>2</sub>O situés dans l'interfeuillelet. D'après les résultats des affinements, le site Pb(1) dans les cristaux naturels est typiquement déficitaire, contenant entre 71 et 100%, tandis que le taux d'occupation de Pb(2) est environ 100% dans les cristaux étudiés. Dans le cristal synthétique que nous avons caractérisé, les sites Pb(1) et Pb(2) ont une occupation de 13 et 87%, respectivement. L'augmentation de la teneur en Pb mène à une légère augmentation du paramètre  $a$ , et une diminution beaucoup plus importante des paramètres  $b$  et  $c$ , ainsi que du volume de la maille. La substitution  $O^{2-} \leftrightarrow (OH)^-$  à deux sites anioniques [O(12) et O(15)] dans le feuillet de polyèdres à uranyle assure un équilibre des charges en conséquence de la variation de la teneur des cations dans l'interfeuillelet. La formule structurale de la fourmariérite peut s'écrire  $Pb_{1-x}[(UO_2)_4O_{3-2x}(OH)_{4+2x}](H_2O)_4$ ,  $Z = 8$ , les composants du feuillet de polyèdres à uranyle étant entre crochets.

(Traduit par la Rédaction)

*Mots-clés:* fourmariérite, minéral à uranyle, détermination de la structure, chimie cristalline.

<sup>§</sup> E-mail address: pburns@nd.edu

## INTRODUCTION

Renewed interest in uranyl minerals results in part from their significance in environmental issues (Finn *et al.* 1996, Wronkiewicz *et al.* 1996, Buck *et al.* 1998, Abdelouas *et al.* 1999). Pb uranyl oxide hydrates as a group form from the oxidation of geologically old uraninite, because of the buildup of radiogenic Pb (Frondele 1958, Finch & Ewing 1992). Seven Pb uranyl oxide hydrate minerals have been described (Table 1). Of these, fourmarierite is of particular interest because of its structural similarity to schoepite (Finch *et al.* 1996), which is present in the oxidation products of primary uraninite (Finch & Ewing 1992), and may also form by alteration of nuclear waste in a geological repository.

The understanding of uranyl structures has been enhanced by the recent application of CCD-based area detectors of X-rays to mineralogical research (Burns 1997, 1998a, b, c, 1999, 2000a, b, Burns & Finch 1999, Burns & Hanchar 1999, Hill & Burns 1999, Burns & Hill 2000a, b, Burns *et al.* 2000). This approach has been particularly successful in the case of Pb uranyl oxide hydrates, with the solutions of the structures of masuyite (Burns & Hanchar 1999), vandendriesscheite (Burns 1997), richetite (Burns 1998a), and wölsendorfite (Burns 1999). Previously, the structures were reported for fourmarierite (Piret 1985), sayrite (Piret *et al.* 1983) and curite (Taylor *et al.* 1981).

Natural Pb uranyl oxide hydrates possess fascinating structures composed of sheets of uranyl polyhedra; they exhibit variable contents of the interlayer, perhaps depending upon the age of the primary uraninite and the nature of the alteration processes. A thorough understanding of the crystal chemistry of these minerals has not yet been attained, but such details are essential to establish an understanding of the relationships between the structures of these minerals and their paragenesis. We have undertaken a systematic study of the crystal chemistry of Pb uranyl oxide hydrates. In the first paper in a series, we report the results on our studies of curite (Li & Burns 2000a). In this contribution, the second in the series, we present data for thirteen crystals of fourmarierite. The primary motivation of the current work is to determine the extent of Pb variation in

fourmarierite, and to develop an understanding of the crystal-chemical mechanisms by which such variation occurs.

## PREVIOUS STUDY

The structure of fourmarierite was reported for a crystal from Shinkolobwe by Piret (1985). On the basis of the structure determination, the formula of fourmarierite was given as  $\text{Pb}[(\text{UO}_2)_4\text{O}_3(\text{OH})_4](\text{H}_2\text{O})_4$ . The structure contains two symmetrically independent Pb sites, both of which were reported to be fully occupied.

## EXPERIMENTAL METHODS

Specimens containing fourmarierite were provided by the Canadian Museum of Nature, the Royal Ontario Museum, and Prof. Rodney C. Ewing, University of Michigan. In addition, we were able to synthesize crystals of fourmarierite suitable for single-crystal study.

*Synthesis of crystals*

Crystals of fourmarierite were synthesized using hydrothermal techniques. A solution was prepared with 0.4 M uranyl nitrate and PbO, with a Pb:U ratio of 1:8. The pH of the solution was adjusted using 1 M NaOH solution to 3.2. The reactants were transferred to a Teflon-lined Parr bomb that was placed in an oven and heated at 200°C for 14 days. The resulting precipitate was recovered by filtration, and contained crystals of fourmarierite and a new Pb uranyl oxide hydrate that is described by Li & Burns (2000b).

*X-ray diffraction*

Well-formed platy crystals of fourmarierite were chosen for X-ray-diffraction experiments. Single-crystal diffraction data were collected for each crystal using MoK $\alpha$  X-radiation and a CCD-based detector mounted on a Bruker three-circle diffractometer. Localities and sizes of the crystals, as well as details of the data collections, are listed in Table 2. The data were integrated and corrected for Lorentz, polarization, and background

TABLE 1. CRYSTALLOGRAPHIC AND COMPOSITIONAL DATA OF Pb URANYL OXIDE HYDRATE MINERALS

Pb-UOH minerals	Structural formula	S.G.	<i>a</i> (Å)	<i>b</i> (Å)	<i>c</i> (Å)	$\alpha$ (°)	$\beta$ (°)	$\gamma$ (°)	Pb/U
wölsendorfite <sup>[1]</sup>	$\text{Pb}_{6.16}\text{Ba}_{0.36}[(\text{UO}_2)_{14}\text{O}_{19}(\text{OH})_4](\text{H}_2\text{O})_{12}$	<i>Cmcm</i>	14.131	13.885	55.969				1:2.15
sayrite <sup>[2]</sup>	$\text{Pb}_2[(\text{UO}_2)_5\text{O}_6(\text{OH})_2](\text{H}_2\text{O})_4$	<i>P2_1/c</i>	10.704	6.960	14.533		116.81		1:2.5
curite <sup>[3]</sup>	$\text{Pb}_3[(\text{UO}_2)_8\text{O}_8(\text{OH})_6](\text{H}_2\text{O})_3$	<i>Pnam</i>	12.551	13.003	8.390				1:2.67
masuyite <sup>[4]</sup>	$\text{Pb}[(\text{UO}_2)_3\text{O}_3(\text{OH})_2](\text{H}_2\text{O})_3$	<i>Pn</i>	12.241	7.008	6.983		90.402		1:3
fourmarierite <sup>[5]</sup>	$\text{Pb}[(\text{UO}_2)_4\text{O}_3(\text{OH})_4](\text{H}_2\text{O})_4$	<i>Bb2_1m</i>	13.986	16.400	14.293				1:4.0
richetite <sup>[6]</sup>	$\text{M}_x\text{Pb}_{8.57}[(\text{UO}_2)_{18}\text{O}_{18}(\text{OH})_{12}](\text{H}_2\text{O})_{41}$	<i>P1</i>	20.9391	12.1000	16.3450	103.87	115.37	90.27	1:4.15
vandendriesscheite <sup>[7]</sup>	$\text{Pb}_{1.57}[(\text{UO}_2)_{10}\text{O}_6(\text{OH})_{11}](\text{H}_2\text{O})_{11}$	<i>Pbca</i>	14.1165	41.478	14.5347				1:6.36

[1] Burns (1999); [2] Piret *et al.* (1983); [3] Taylor *et al.* (1981); [4] Burns & Hanchar (1999); [5] Piret (1985); [6] Burns (1998a);

[7] Burns (1997)

TABLE 2. INFORMATION FOR CRYSTALS OF FOURMARIERITE STUDIED

Samples*	Locality*	Crystal size (mm)	Frame width (in $\phi$ )	Exposure time (s/frame)
CMNMC81096	Shinkolobwe	0.14×0.07×0.06	0.3	30
CMNMC81097	Shinkolobwe	0.18×0.08×0.02	0.3	30
CMNMC81098	Shinkolobwe	0.18×0.08×0.02	0.3	30
CMNMC81099	Shinkolobwe	0.12×0.10×0.04	0.3	20
CMNMC81100	Shinkolobwe	0.14×0.12×0.08	0.3	20
CMNMC53066	Shinkolobwe	0.14×0.14×0.04	0.3	20
M30767	Shinkolobwe	0.16×0.07×0.04	0.3	15
M31669	Shinkolobwe	0.21×0.18×0.06	0.3	10
CMNMC81103	Shinkolobwe	0.20×0.14×0.02	0.3	35
UMN753			0.3	
UMN486	Shaba	0.08×0.08×0.01	0.3	
CMNMC81101	Shaba		0.3	60
Synthetic		0.05×0.04×0.01	0.3	120

\* Sources of samples: UNM: Prof. Rodney C. Ewing; CMNMC: Canadian Museum of Nature; M: Royal Ontario Museum

\* Localities: Shinkolobwe, Shaba, Democratic Republic of Congo; Shaba, Democratic Republic of Congo

effects using the Bruker program SAINT. Each dataset was corrected for absorption. Where well-developed faces bounded the crystals, Gaussian interpolation was used, but where crystal faces were less well developed, semi-empirical corrections were done on the basis of equivalent reflections. The structures were refined on the basis of  $F^2$  for all unique data in space group  $Bb2_1m$  using the SHELXTL software package. Refinement began with isotropic displacement parameters for all atoms, followed by conversion to anisotropic displacement parameters for U and Pb atoms. The final cycles of refinement included the Pb site-occupancies, and resulted in agreement indices ( $R1$ ) ranging from 3.6% to 6.2%, calculated for observed ( $|F_o| \geq 4\sigma_F$ ) reflections (Table 3). The highest  $R$  was obtained for the synthetic crystal, which was substantially smaller than the others (Table 2). Unit-cell parameters and Pb occupancies derived from site-scattering refinement for each crystal

are given in Table 3, together with the corresponding final agreement index ( $R1$ ). Final atomic coordinates are in Table 4, and selected interatomic distances are in Table 5.

### Electron-microprobe analyses

With the exception of the synthetic crystal, the fourmarierite crystals selected for our X-ray-diffraction investigation were mounted at the center of hollow aluminum tubes using epoxy. Each crystal was hand-polished and coated with carbon. The elemental concentrations were analyzed using an electron microprobe (JEOL Superprobe 733 at the Canadian Museum of Nature) equipped with four wavelength-dispersion spectrometers and operated at 15 kV. A beam current of 20 nA and a beam diameter of 20  $\mu\text{m}$  were used. Synthetic  $\text{UO}_2$  and crocoite were used as standards for U and Pb, respectively. We sought Na, K, Ca, Sr, Ba, and Th, but no significant concentrations were found. The analyses were done with 25 s spent counting for each element, using the Tracor Northern Program 5500 and 5600 software, and the ZAF correction using the PAP correction program (C. Davidson, CSIRO, pers. commun.). Several different points were analyzed for each crystal, depending on the size of the crystal examined. No significant chemical zoning was observed in electron-back-scatter images of any crystals of fourmarierite examined. The results of the chemical analyses are given in Table 6, with the proportion of  $\text{H}_2\text{O}$  assumed on the basis of stoichiometry.

## RESULTS

### Cation polyhedra

The structure of fourmarierite contains four symmetrically unique U sites. All of the  $\text{U}^{6+}$  cations are strongly bonded to two atoms of O (designated  $\text{O}_{U1}$ ),

TABLE 3. UNIT-CELL PARAMETERS AND Pb OCCUPANCY FROM REFINEMENTS OF VARIOUS CRYSTALS OF FOURMARIERITE

Samples	$a$ (Å)	$b$ (Å)	$c$ (Å)	# ref. for unit cell	$R1$ (%)	# $F > 4\sigma_F$	Pb(1)	Pb(2)	Total Pb
CMNMC81096	14.010(1)	16.401(1)	14.317(1)	5363	4.64	3156	0.495(3)	0.527(3)	1.022
CMNMC81097	14.014(1)	16.419(1)	14.330(1)	5864	5.42	3284	0.469(4)	0.513(4)	0.982
CMNMC81098	14.013(1)	16.420(1)	14.329(1)	5299	3.57	2506	0.433(2)	0.503(2)	0.936
CMNMC81099	14.014(1)	16.412(1)	14.322(1)	4049	4.82	2817	0.476(3)	0.521(3)	0.997
CMNMC81100	14.022(1)	16.450(1)	14.355(1)	5358	5.11	3067	0.412(3)	0.507(3)	0.919
CMNMC53066	14.020(1)	16.441(1)	14.348(1)	4977	5.33	2463	0.406(4)	0.501(4)	0.907
M30767	14.020(1)	16.425(1)	14.334(1)	4282	4.39	2614	0.448(3)	0.505(3)	0.953
M31669	14.000(1)	16.417(1)	14.357(1)	3589	5.24	2419	0.394(3)	0.501(3)	0.895
CMNMC81103	14.018(1)	16.468(1)	14.368(1)	7566	4.34	3372	0.366(3)	0.497(3)	0.863
UMN753	14.024(2)	16.420(1)	14.338(1)	3609	5.80	3367	0.453(5)	0.507(5)	0.960
UMN486	14.010(1)	16.468(1)	14.369(1)	4826	5.64	2401	0.355(4)	0.500(4)	0.855
CMNMC81101	14.026(1)	16.476(1)	14.382(1)	7117	5.49	3467	0.363(3)	0.505(3)	0.868
Synthetic	13.938(2)	16.638(3)	14.672(2)	1264	6.18	1431	0.063(5)	0.434(4)	0.497
Piret (1985)	13.986(4)	16.400(5)	14.293(9)		4.60	2750	0.5	0.5	1.00

TABLE 4. ATOMIC COORDINATES ( $\times 10^4$ ) AND EQUIVALENT ISOTROPIC DISPLACEMENT PARAMETERS ( $\text{\AA}^2 \times 10^3$ ) FOR FOURMARIERITE CRYSTALS

	CMCNC 81096	CMCNC 81097	CMNMC 81098	CMNMC 81099	CMNMC 81100	CMNMC 53066	M30767	M31669	CMNMC 81103	UMN753	UMN486	CMNMC 81101	Synthetic
U(1)	<i>x</i>	251(1)	250(1)	248(1)	250(1)	249(1)	249(1)	241(1)	248(1)	248(1)	247(1)	249(1)	229(1)
	<i>y</i>	1170(1)	1170(1)	1168(1)	1169(1)	1167(1)	1168(1)	1170(1)	1171(1)	1166(1)	1166(1)	1166(1)	1146(1)
	<i>z</i>	2427(1)	2430(1)	2432(1)	2430(1)	2433(1)	2432(1)	2431(1)	2433(1)	2432(1)	2433(1)	2433(1)	2292(1)
	$U_{eq}$	15(1)	24(1)	14(1)	13(1)	12(1)	14(1)	11(1)	17(1)	13(1)	16(1)	15(1)	24(1)
U(2)	<i>x</i>	156(1)	154(1)	153(1)	154(1)	151(1)	151(1)	154(1)	154(1)	150(1)	154(1)	149(1)	99(2)
	<i>y</i>	3827(1)	3829(1)	3830(1)	3828(1)	3831(1)	3831(1)	3830(1)	3832(1)	3833(1)	3830(1)	3834(1)	3872(1)
	<i>z</i>	2394(1)	2398(1)	2400(1)	2397(1)	2402(1)	2403(1)	2401(1)	2404(1)	2403(1)	2400(1)	2405(1)	2318(2)
	$U_{eq}$	15(1)	24(1)	14(1)	14(1)	11(1)	14(1)	10(1)	16(1)	13(1)	16(1)	14(1)	25(1)
U(3)	<i>x</i>	2724(1)	2723(1)	2723(1)	2724(1)	2724(1)	2723(1)	2723(1)	2722(1)	2725(1)	2724(1)	2725(1)	2724(1)
	<i>y</i>	213(1)	213(1)	214(1)	214(1)	216(1)	217(1)	213(1)	216(1)	221(1)	214(1)	221(1)	220(1)
	<i>z</i>	2215(1)	2215(1)	2215(1)	2215(1)	2213(1)	2214(1)	2216(1)	2212(1)	2211(1)	2216(1)	2213(1)	2187(1)
	$U_{eq}$	14(1)	23(1)	14(1)	12(1)	11(1)	14(1)	10(1)	16(1)	12(1)	16(1)	14(1)	22(1)
U(4)	<i>x</i>	2416(1)	2415(1)	2417(1)	2416(1)	2417(1)	2417(1)	2415(1)	2415(1)	2420(1)	2413(1)	2419(1)	2420(1)
	<i>y</i>	2536(1)	2535(1)	2534(1)	2536(1)	2533(1)	2533(1)	2536(1)	2531(1)	2532(1)	2534(1)	2530(1)	2532(1)
	<i>z</i>	2613(1)	2614(1)	2615(1)	2616(1)	2616(1)	2616(1)	2615(1)	2603(1)	2616(1)	2613(1)	2616(1)	2670(1)
	$U_{eq}$	15(1)	24(1)	15(1)	13(1)	12(1)	15(1)	11(1)	18(1)	14(1)	16(1)	15(1)	22(1)
Pb(1)	<i>x</i>	1877(1)	1870(1)	1870(1)	1874(1)	1869(1)	1869(1)	1871(1)	1860(2)	1869(1)	1868(1)	1870(2)	1871(1)
	<i>y</i>	3817(1)	3816(1)	3817(1)	3821(1)	3814(2)	3811(2)	3822(2)	3810(2)	3809(1)	3816(2)	3814(2)	3806(1)
	<i>z</i>	0	0	0	0	0	0	0	0	0	0	0	0
	$U_{eq}$	28(1)	38(1)	27(1)	28(1)	25(1)	28(1)	23(1)	29(1)	28(1)	29(1)	30(1)	73(14)
Pb(2)	<i>x</i>	3299(1)	3291(1)	3288(1)	3293(1)	3283(1)	3282(1)	3291(1)	3277(1)	3274(1)	3289(1)	3274(1)	3275(1)
	<i>y</i>	6038(1)	6036(1)	6034(1)	6038(1)	6034(1)	6034(1)	6041(1)	6040(1)	6032(1)	6037(1)	6032(2)	6030(1)
	<i>z</i>	0	0	0	0	0	0	0	0	0	0	0	0
	$U_{eq}$	28(1)	36(1)	26(1)	26(1)	24(1)	27(1)	22(1)	30(1)	26(1)	29(1)	28(1)	28(1)
O(1)	<i>x</i>	-43(14)	-54(15)	-23(10)	-36(15)	-34(15)	-64(14)	-22(13)	-43(17)	-42(12)	-35(17)	-56(17)	-57(12)
	<i>y</i>	1339(11)	1363(11)	1397(9)	1341(12)	1383(12)	1397(14)	1342(13)	1327(14)	1367(10)	1386(14)	1340(16)	1353(10)
	<i>z</i>	1229(12)	1255(13)	1231(10)	1226(13)	1246(11)	1238(13)	1243(10)	1236(14)	1227(10)	1217(16)	1249(16)	1230(11)
	$U_{eq}$	27(4)	36(4)	26(3)	29(4)	24(4)	21(4)	23(4)	31(5)	25(3)	23(4)	23(5)	42(8)
O(2)	<i>x</i>	522(12)	506(13)	512(8)	525(12)	516(13)	502(13)	515(11)	516(15)	535(11)	489(16)	518(15)	571(11)
	<i>y</i>	940(11)	964(10)	1018(9)	951(11)	959(13)	963(13)	923(11)	946(14)	944(9)	933(13)	950(15)	938(9)
	<i>z</i>	3665(12)	3655(14)	3655(10)	3649(14)	3662(13)	3670(14)	3646(10)	3637(15)	3658(10)	3674(18)	3661(15)	3638(12)
	$U_{eq}$	27(4)	34(4)	20(3)	23(4)	28(5)	22(4)	16(4)	29(5)	23(3)	26(5)	18(5)	25(3)
O(3)	<i>x</i>	562(10)	560(12)	534(8)	540(12)	550(12)	571(12)	540(11)	567(13)	547(11)	558(14)	530(16)	539(10)
	<i>y</i>	3752(10)	3753(10)	3794(9)	3741(10)	3746(12)	3773(14)	3715(11)	3744(13)	3754(10)	3765(12)	3765(17)	3759(9)
	<i>z</i>	1187(10)	1186(12)	1195(9)	1198(12)	1192(11)	1219(13)	1183(9)	1176(12)	1201(10)	1209(15)	1207(16)	1198(11)
	$U_{eq}$	19(3)	29(4)	23(3)	19(4)	20(4)	23(5)	18(4)	22(4)	26(3)	18(4)	25(5)	23(3)
O(4)	<i>x</i>	-309(12)	-299(12)	-282(9)	-276(12)	-301(12)	-293(14)	-299(11)	-305(14)	-293(11)	-310(16)	-308(19)	-299(11)
	<i>y</i>	3857(12)	3865(10)	3915(9)	3873(12)	3876(13)	3882(16)	3811(13)	3852(15)	3871(10)	3878(14)	3870(20)	3872(9)
	<i>z</i>	3577(12)	3617(12)	3584(10)	3552(14)	3574(12)	3576(15)	3576(10)	3558(14)	3571(10)	3560(17)	3553(19)	3559(11)
	$U_{eq}$	33(4)	32(4)	33(4)	28(5)	26(4)	33(5)	28(4)	34(5)	26(3)	27(5)	40(7)	26(3)
O(5)	<i>x</i>	2913(10)	2903(11)	2875(8)	2903(11)	2913(11)	2899(12)	2907(10)	2920(12)	2908(10)	2924(13)	2902(14)	2900(10)
	<i>y</i>	270(11)	256(11)	295(10)	272(13)	262(16)	234(12)	260(14)	256(10)	268(12)	270(16)	280(9)	298(10)
	<i>z</i>	970(11)	977(12)	970(10)	981(13)	968(11)	935(14)	970(10)	982(12)	974(10)	963(15)	975(15)	963(11)
	$U_{eq}$	19(3)	29(3)	24(3)	21(4)	19(4)	23(4)	18(4)	19(4)	22(3)	14(4)	20(5)	19(3)
O(6)	<i>x</i>	2454(12)	2455(11)	2474(8)	2472(14)	2436(12)	2459(13)	2460(11)	2466(15)	2460(11)	2471(15)	2476(17)	2435(12)
	<i>y</i>	68(10)	88(9)	145(8)	103(12)	102(12)	110(14)	50(12)	130(15)	118(9)	131(12)	138(17)	124(10)
	<i>z</i>	3458(11)	3461(11)	3433(9)	3417(14)	3444(11)	3446(13)	3450(10)	3391(14)	3435(10)	3437(17)	3440(16)	3430(13)
	$U_{eq}$	24(4)	23(3)	19(3)	33(5)	20(4)	22(4)	18(4)	35(5)	22(3)	20(5)	27(6)	29(4)
O(7)	<i>x</i>	2526(11)	2529(13)	2505(8)	2527(11)	2516(12)	2515(14)	2504(11)	2526(14)	2532(11)	2520(16)	2520(14)	2508(11)
	<i>y</i>	2924(11)	2936(12)	2954(9)	2946(10)	2943(13)	2940(16)	2885(11)	2905(14)	2930(10)	2921(14)	2897(15)	2919(10)
	<i>z</i>	1423(12)	1411(15)	1428(11)	1445(14)	1441(13)	1435(16)	1418(12)	1446(16)	1455(10)	1414(18)	1428(16)	1449(12)
	$U_{eq}$	23(4)	37(4)	25(3)	19(4)	24(4)	30(5)	19(4)	28(5)	21(3)	23(5)	17(5)	24(3)
O(8)	<i>x</i>	2383(12)	2395(14)	2394(9)	2384(13)	2388(15)	2390(15)	2399(12)	2391(15)	2405(12)	2403(18)	2415(16)	2395(12)
	<i>y</i>	2160(11)	2170(12)	2215(9)	2155(11)	2174(14)	2202(18)	2140(12)	2157(14)	2153(11)	2179(16)	2158(16)	2160(11)
	<i>z</i>	3801(12)	3814(16)	3836(11)	3820(14)	3835(15)	3827(17)	3828(11)	3786(15)	3803(11)	3840(20)	3819(17)	3798(13)
	$U_{eq}$	23(4)	42(5)	28(3)	28(5)	35(5)	37(6)	25(4)	31(5)	26(3)	33(6)	23(5)	28(4)
O(9)	<i>x</i>	1072(10)	1080(10)	1075(7)	1071(10)	1071(10)	1065(11)	1082(10)	1098(12)	1060(9)	1096(14)	1071(14)	1055(9)
	<i>y</i>	-167(10)	-161(9)	-104(8)	-175(9)	-154(10)	-138(13)	-184(11)	-186(12)	-150(8)	-146(12)	-146(14)	-152(8)
	<i>z</i>	1922(11)	1955(11)	1931(9)	1929(11)	1946(10)	1946(13)	1937(10)	1903(13)	1933(8)	1945(16)	1934(15)	1946(10)
	$U_{eq}$	17(3)	19(3)	14(3)	6(3)	10(3)	16(4)	14(4)	18(4)	11(2)	18(4)	15(5)	13(3)

resulting in approximately linear uranyl ions with  $\langle U-O_{Ur} \rangle \approx 1.8 \text{ \AA}$ , as is typically observed in the structure of  $U^{6+}$ -bearing phases (Burns *et al.* 1997a). Each  $U^{6+}$  cation is coordinated by five additional anions, forming  $Ur\phi_5$  pentagonal bipyramids [ $Ur$ :  $(UO_2)^{2+}$  uranyl ion,  $\phi$ : unspecified ligand]. For the natural crystals,  $\langle U(1)-5\phi_{eq} \rangle$ ,  $\langle U(2)-5\phi_{eq} \rangle$ ,  $\langle U(3)-5\phi_{eq} \rangle$ , and  $\langle U(4)-5\phi_{eq} \rangle$  range from 2.35 to 2.38, 2.35 to 2.37, 2.37 to 2.40, and 2.35 to 2.37  $\text{\AA}$ , respectively. In the case of the syn-

thetic crystal, which has much less Pb than the natural crystals, the average bond-lengths of the uranyl polyhedra are 2.36, 2.43, 2.40 and 2.38  $\text{\AA}$  for the U(1), U(2), U(3) and U(4) polyhedra, respectively.

There are two distinct Pb sites, and eight symmetrically distinct  $H_2O$  sites in the interlayer of the structure of fourmarierite. In the natural crystals, Pb(1) is coordinated by four  $O_{Ur}$  atoms and three  $H_2O$  groups, with  $\langle Pb(1)-\phi \rangle$  ranging from 2.68 to 2.72  $\text{\AA}$ . Pb(2)

	CMCNC 81096	CMCNC 81097	CMNMC 81098	CMNMC 81099	CMNMC 81100	CMNMC 53066	M30767	M31669	CMNMC 81103	UMN753	UMN486	CMNMC 81101	Synthetic
O(10)													
<i>x</i>	-731(12)	-741(13)	-728(9)	-726(12)	-738(13)	-749(12)	-733(11)	-732(14)	-738(10)	-738(16)	-748(17)	-729(13)	-779(17)
<i>y</i>	91(11)	84(10)	127(8)	74(10)	97(12)	111(14)	57(11)	80(13)	85(9)	93(13)	88(17)	86(11)	175(15)
<i>z</i>	2420(12)	2425(12)	2415(9)	2401(12)	2442(11)	2438(12)	2436(10)	2448(13)	2437(9)	2415(15)	2463(16)	2444(12)	2349(16)
<i>U<sub>eq</sub></i>	25(4)	28(4)	18(3)	15(4)	18(4)	15(4)	15(4)	24(5)	18(3)	18(4)	23(5)	29(4)	14(6)
O(11)													
<i>x</i>	-1311(11)	-1330(12)	-1329(8)	-1336(11)	-1324(12)	-1327(13)	-1327(1)	-1329(1)	-1321(9)	-1318(14)	-1324(15)	-1324(10)	-1327(17)
<i>y</i>	1612(10)	1598(9)	1616(8)	1590(10)	1599(12)	1603(14)	1573(11)	1591(13)	1593(8)	1584(12)	1573(15)	1596(8)	1639(16)
<i>z</i>	2889(11)	2900(12)	2894(10)	2899(13)	2868(12)	2888(14)	2879(11)	2906(14)	2880(8)	2862(15)	2865(16)	2890(10)	2752(22)
<i>U<sub>eq</sub></i>	17(3)	23(3)	15(3)	14(4)	20(4)	20(4)	16(4)	23(5)	10(2)	15(4)	18(5)	15(3)	25(7)
O(12)													
<i>x</i>	699(15)	704(15)	680(9)	695(12)	688(16)	692(16)	688(12)	694(15)	665(12)	666(19)	659(18)	694(13)	629(17)
<i>y</i>	2493(15)	2533(13)	2575(9)	2502(12)	2528(16)	2550(19)	2493(15)	2493(17)	2517(12)	2543(17)	2527(19)	2538(11)	2546(20)
<i>z</i>	2687(14)	2702(14)	2715(10)	2699(13)	2690(14)	2677(15)	2690(11)	2686(15)	2741(10)	2742(19)	2754(16)	2725(12)	2712(18)
<i>U<sub>eq</sub></i>	42(5)	43(4)	26(3)	24(6)	40(5)	38(6)	29(4)	37(5)	31(3)	36(6)	32(6)	29(4)	24(6)
O(13)													
<i>x</i>	1795(13)	1824(15)	1811(9)	1802(14)	1809(14)	1813(16)	1814(12)	1816(15)	1791(12)	1817(15)	1817(17)	1804(12)	1820(19)
<i>y</i>	1344(11)	1344(11)	1379(8)	1342(10)	1355(12)	1341(15)	1314(11)	1330(12)	1355(10)	1360(12)	1342(15)	1342(9)	1443(15)
<i>z</i>	2144(13)	2144(15)	2156(11)	2135(14)	2158(13)	2170(16)	2188(11)	2154(15)	2129(11)	2141(16)	2173(16)	2172(11)	2075(19)
<i>U<sub>eq</sub></i>	28(4)	36(4)	25(3)	24(5)	25(5)	30(5)	22(4)	26(5)	26(3)	16(4)	22(5)	22(3)	21(7)
O(14)													
<i>x</i>	-1156(13)	-1165(12)	-1163(8)	-1167(13)	-1176(13)	-1192(15)	-1165(1)	-1173(1)	-1171(10)	-1187(13)	-1150(13)	-1164(11)	-1154(19)
<i>y</i>	3115(11)	3132(10)	3161(8)	3144(11)	3164(12)	3149(15)	3105(12)	3125(12)	3125(8)	3119(10)	3098(12)	3116(8)	3171(17)
<i>z</i>	1878(13)	1899(13)	1885(9)	1863(13)	1898(12)	1905(15)	1913(11)	1922(12)	1896(9)	1886(14)	1904(13)	1902(11)	1780(16)
<i>U<sub>eq</sub></i>	28(4)	28(4)	17(3)	23(4)	23(4)	29(5)	24(4)	17(4)	16(3)	8(3)	8(4)	20(3)	15(6)
O(15)													
<i>x</i>	1825(11)	1823(13)	1828(8)	1825(11)	1819(13)	1829(13)	1831(11)	1838(14)	1816(12)	1837(16)	1828(16)	1841(12)	1832(19)
<i>y</i>	3816(12)	3833(12)	3870(10)	3815(12)	3821(14)	3838(17)	3791(14)	3816(15)	3834(12)	3848(16)	3834(18)	3841(11)	3883(20)
<i>z</i>	2985(11)	2985(13)	2997(10)	3001(12)	2991(12)	2980(14)	2979(10)	3003(13)	3002(11)	2961(17)	2999(16)	3001(12)	3058(18)
<i>U<sub>eq</sub></i>	24(4)	33(4)	25(3)	19(4)	28(4)	26(5)	23(4)	26(4)	29(3)	25(5)	24(5)	27(3)	33(7)
O(16)													
<i>x</i>	1310(20)	1350(30)	1302(16)	1320(20)	1340(20)	1350(30)	1352(19)	1400(30)	1317(19)	1270(30)	1370(30)	1300(19)	1428(40)
<i>y</i>	5396(17)	5418(19)	5481(14)	5408(16)	5450(20)	5470(30)	5429(18)	5520(30)	5478(15)	5400(30)	5460(20)	5485(15)	5397(35)
<i>z</i>	0	0	0	0	0	0	0	0	0	0	0	0	0
<i>U<sub>eq</sub></i>	35(7)	58(9)	43(7)	31(8)	49(10)	60(12)	31(7)	71(14)	33(6)	51(12)	29(9)	35(6)	86(21)
O(17)													
<i>x</i>	3708(17)	3723(19)	3710(14)	3703(19)	3710(20)	3710(20)	3722(18)	3690(20)	3705(16)	3680(20)	3690(30)	3713(17)	3312(37)
<i>y</i>	4500(15)	4521(14)	4539(13)	4484(16)	4541(19)	4537(19)	4483(17)	4500(20)	4530(14)	4507(16)	4500(20)	4531(13)	4190(30)
<i>z</i>	0	0	0	0	0	0	0	0	0	0	0	0	0
<i>U<sub>eq</sub></i>	25(6)	35(6)	32(6)	29(7)	35(8)	26(7)	27(7)	34(8)	26(5)	14(6)	33(9)	27(5)	55(16)
O(18)													
<i>x</i>	1360(20)	1370(20)	1358(16)	1360(20)	1360(20)	1430(30)	1360(20)	1340(30)	1440(20)	1390(50)	1410(30)	1420(20)	1667(45)
<i>y</i>	2121(19)	2150(20)	2195(16)	2140(20)	2150(20)	2150(30)	2160(20)	2120(30)	2120(20)	2130(40)	2140(30)	2119(19)	2000(38)
<i>z</i>	0	0	0	0	0	0	0	0	0	0	0	0	0
<i>U<sub>eq</sub></i>	39(7)	54(8)	52(7)	57(10)	40(8)	51(10)	48(9)	61(12)	53(8)	82(18)	45(11)	52(8)	91(23)
O(19)													
<i>x</i>	4510(40)	4540(40)	4577(18)	4630(30)	4600(30)	4550(30)	4570(30)	4540(40)	4600(30)	4530(40)	4590(50)	4590(30)	5352(45)
<i>y</i>	7250(40)	7330(30)	7380(17)	7340(30)	7320(30)	7340(30)	7320(30)	7300(40)	7320(20)	7360(30)	7370(40)	7327(18)	7220(39)
<i>z</i>	0	0	0	0	0	0	0	0	0	0	0	0	0
<i>U<sub>eq</sub></i>	150(20)	95(15)	68(9)	111(18)	87(15)	65(12)	90(13)	110(20)	69(10)	59(13)	90(20)	62(10)	102(24)
O(20)													
<i>x</i>	1200(20)	1160(20)	1173(16)	1180(20)	1190(20)	1180(20)	1215(19)	1200(30)	1140(30)	1160(40)	1130(30)	1140(20)	1367(35)
<i>y</i>	-400(20)	-397(19)	-380(16)	-425(18)	-400(20)	-380(20)	-471(18)	-410(30)	-410(20)	-400(30)	-390(30)	-398(19)	-501(33)
<i>z</i>	0	0	0	0	0	0	0	0	0	0	0	0	0
<i>U<sub>eq</sub></i>	49(9)	56(9)	53(8)	41(9)	38(8)	40(9)	37(8)	62(13)	63(10)	59(14)	37(10)	59(10)	54(16)
O(21)													
<i>x</i>	3580(20)	3540(30)	3553(15)	3570(20)	3550(20)	3560(20)	3550(17)	3570(20)	3570(20)	3540(20)	3570(30)	3590(20)	4801(26)
<i>y</i>	1650(20)	1700(20)	1729(15)	1676(19)	1700(20)	1680(20)	1661(18)	1650(20)	1722(17)	1724(18)	1750(30)	1723(18)	107(25)
<i>z</i>	0	0	0	0	0	0	0	0	0	0	0	0	0
<i>U<sub>eq</sub></i>	52(9)	58(9)	41(6)	45(9)	37(8)	38(9)	25(7)	42(10)	40(6)	20(7)	35(10)	46(7)	29(10)
O(22)													
<i>x</i>	960(20)	920(20)	912(15)	920(20)	930(20)	940(20)	893(19)	1000(30)	900(18)	920(30)	850(30)	910(20)	912(31)
<i>y</i>	7730(20)	7748(17)	7780(13)	7728(19)	7739(19)	7780(20)	7754(18)	7790(30)	7735(15)	7710(30)	7700(30)	7760(16)	7656(30)
<i>z</i>	0	0	0	0	0	0	0	0	0	0	0	0	0
<i>U<sub>eq</sub></i>	52(9)	48(7)	40(6)	55(10)	37(8)	36(8)	37(8)	68(13)	34(5)	52(11)	39(10)	42(7)	43(13)
O(23)													
<i>x</i>	3250(30)	3240(30)	3292(19)	3220(30)	3210(30)	3210(30)	3210(30)	3170(30)	3260(30)	3260(30)	3240(40)	3150(40)	3642(30)
<i>y</i>	8680(30)	8730(30)	8756(19)	8690(30)	8750(30)	8710(30)	8680(30)	8690(20)	8710(20)	8740(30)	8730(40)	8670(30)	8824(30)
<i>z</i>	0	0	0	0	0	0	0	0	0	0	0	0	0
<i>U<sub>eq</sub></i>	85(14)	80(12)	76(10)	93(15)	75(13)	59(12)	74(12)	47(10)	60(9)	49(11)	76(18)	105(17)	46(14)

is coordinated by six  $O_{Ur}$  atoms and three  $H_2O$  groups, with  $\langle Pb(2)-\phi \rangle$  ranging from 2.72 to 2.75 Å (Table 5, Fig. 1). The coordination polyhedron about the Pb(1) site in the synthetic crystal is similar to those in the natural crystals, although it is only 13% occupied, with a  $\langle Pb(1)-\phi \rangle$  bond length of 2.62 Å. The coordination polyhedron about Pb(2) in the synthetic crystal, which is 87% occupied, is not identical to those in the natural crystals. The  $H_2O(19)$  and  $H_2O(21)$  groups assume different positions in the interlayer of the synthetic crystal, resulting in the addition of  $H_2O(19)$  and removal of  $H_2O(21)$  from the Pb(2) coordination polyhedron.

### Structural connectivity

The  $Ur\phi_5$  pentagonal bipyramids share edges and vertices, forming sheets oriented parallel to (100) (Fig. 2). Symmetrically equivalent sheets are located at  $c \approx 0.25$  and  $c \approx 0.75$  (Fig. 3). In the interlayer, the Pb(1) $\phi_7$  and Pb(2) $\phi_9$  polyhedra share an edge, forming dimers (Fig. 4). Of the eight  $H_2O$  groups, four [O(16), O(17), O(18) and O(19)] are bonded to Pb in the interlayer, and four [O(20), O(21), O(22) and O(23)] are held in the structure by hydrogen bonds only (Fig. 3). Adjacent sheets are connected through bonds to the Pb<sup>2+</sup> cations and the  $H_2O$  groups (Fig. 3).



TABLE 5. SELECTED BOND-DISTANCES (Å) FOR FOURMARIERITE

	CMNMC 81096	CMNMC 81097	CMNMC 81098	CMNMC 81099	CMNMC 81100	CMNMC 53066	M30767	M31669	CMNMC 81103	UMN753	UMN486	CMNMC 81101	Synthetic
U(1)-O(1)	1.79(2)	1.76(2)	1.80(1)	1.79(2)	1.79(2)	1.81(2)	1.77(2)	1.78(2)	1.81(2)	1.82(2)	1.78(2)	1.81(2)	1.72(3)
U(1)-O(2)	1.85(2)	1.82(2)	1.81(1)	1.82(2)	1.84(2)	1.84(2)	1.83(2)	1.81(2)	1.84(2)	1.85(3)	1.84(2)	1.83(2)	1.84(3)
U(1)-O(13)	2.22(2)	2.26(2)	2.25(1)	2.23(2)	2.25(2)	2.24(2)	2.23(2)	2.26(2)	2.23(2)	2.26(2)	2.25(2)	2.23(2)	2.29(3)
U(1)-O(10)	2.24(2)	2.26(2)	2.19(1)	2.26(2)	2.34(2)	2.34(2)	2.29(2)	2.25(2)	2.25(2)	2.24(2)	2.26(3)	2.25(2)	2.14(2)
U(1)-O(12)	2.29(2)	2.36(2)	2.42(2)	2.31(2)	2.35(3)	2.38(3)	2.29(2)	2.29(3)	2.34(2)	2.37(3)	2.36(3)	2.38(2)	2.47(3)
U(1)-O(11)	2.40(2)	2.42(2)	2.42(1)	2.42(2)	2.40(2)	2.41(2)	2.39(2)	2.40(2)	2.40(1)	2.38(2)	2.38(2)	2.41(1)	2.42(3)
U(1)-O(9)	2.58(2)	2.57(1)	2.49(1)	2.59(2)	2.56(2)	2.53(2)	2.61(2)	2.64(2)	2.55(1)	2.56(2)	2.55(2)	2.55(1)	2.49(2)
<U(1)-O <sub>11</sub> >	1.82	1.79	1.81	1.81	1.82	1.83	1.80	1.80	1.83	1.84	1.81	1.82	1.78
<U(1)-φ>	2.35	2.37	2.35	2.36	2.38	2.36	2.36	2.37	2.35	2.36	2.36	2.36	2.36
U(2)-O(4)	1.82(2)	1.86(2)	1.81(1)	1.76(2)	1.80(2)	1.80(2)	1.80(2)	1.78(2)	1.79(2)	1.79(2)	1.77(3)	1.78(2)	1.77(3)
U(2)-O(3)	1.82(2)	1.83(2)	1.81(1)	1.81(2)	1.83(2)	1.80(2)	1.84(1)	1.86(2)	1.82(2)	1.80(2)	1.81(2)	1.82(2)	1.83(3)
U(2)-O(10) <sub>a</sub>	2.23(2)	2.20(2)	2.28(1)	2.20(2)	2.24(2)	2.27(2)	2.17(2)	2.20(2)	2.22(2)	2.23(2)	2.23(3)	2.22(2)	2.37(3)
U(2)-O(14)	2.30(2)	2.29(2)	2.27(1)	2.30(2)	2.28(2)	2.31(2)	2.31(2)	2.30(2)	2.31(1)	2.33(2)	2.30(2)	2.30(2)	2.24(3)
U(2)-O(12)	2.36(2)	2.30(2)	2.24(1)	2.34(2)	2.31(3)	2.27(3)	2.36(2)	2.36(3)	2.34(2)	2.29(3)	2.32(3)	2.31(2)	2.40(3)
U(2)-O(9) <sub>a</sub>	2.48(2)	2.48(2)	2.55(1)	2.47(1)	2.48(2)	2.49(2)	2.46(2)	2.49(2)	2.48(1)	2.51(2)	2.49(2)	2.47(1)	2.49(2)
U(2)-O(15)	2.49(2)	2.49(2)	2.50(1)	2.50(2)	2.49(2)	2.49(2)	2.49(2)	2.51(2)	2.49(2)	2.49(2)	2.50(2)	2.52(2)	2.65(3)
<U(2)-O <sub>11</sub> >	1.82	1.85	1.81	1.78	1.82	1.80	1.82	1.82	1.81	1.80	1.79	1.80	1.80
<U(2)-φ>	2.37	2.35	2.37	2.36	2.36	2.37	2.36	2.37	2.37	2.37	2.37	2.36	2.43
U(3)-O(5)	1.80(2)	1.79(2)	1.80(1)	1.79(2)	1.81(2)	1.85(2)	1.81(1)	1.79(2)	1.80(1)	1.82(2)	1.80(2)	1.82(2)	1.77(3)
U(3)-O(6)	1.84(2)	1.84(2)	1.78(1)	1.77(2)	1.82(2)	1.82(2)	1.83(1)	1.74(2)	1.81(1)	1.79(2)	1.80(2)	1.81(2)	1.86(3)
U(3)-O(10) <sub>b</sub>	2.24(2)	2.22(2)	2.24(1)	2.25(2)	2.22(2)	2.21(2)	2.24(2)	2.23(2)	2.23(2)	2.23(2)	2.20(2)	2.24(2)	2.19(2)
U(3)-O(13)	2.27(2)	2.25(2)	2.30(1)	2.26(2)	2.27(2)	2.25(2)	2.21(2)	2.23(2)	2.28(2)	2.27(2)	2.24(2)	2.26(2)	2.34(3)
U(3)-O(15) <sub>c</sub>	2.39(2)	2.37(2)	2.31(1)	2.40(2)	2.40(2)	2.37(3)	2.43(2)	2.40(2)	2.39(2)	2.34(3)	2.39(3)	2.37(2)	2.40(3)
U(3)-O(9)	2.43(1)	2.41(1)	2.40(1)	2.44(1)	2.43(1)	2.43(2)	2.43(2)	2.41(2)	2.45(1)	2.39(2)	2.43(2)	2.45(1)	2.43(2)
U(3)-O(11) <sub>b</sub>	2.67(2)	2.64(2)	2.66(1)	2.62(2)	2.64(2)	2.64(2)	2.60(0)	2.63(2)	2.63(1)	2.62(2)	2.60(2)	2.63(1)	2.64(3)
<U(3)-O <sub>11</sub> >	1.82	1.82	1.79	1.78	1.82	1.84	1.82	1.77	1.81	1.81	1.80	1.82	1.81
<U(3)-φ>	2.40	2.38	2.38	2.39	2.39	2.38	2.38	2.38	2.40	2.37	2.37	2.39	2.40
U(4)-O(8)	1.81(2)	1.82(2)	1.83(2)	1.83(2)	1.81(2)	1.82(2)	1.86(2)	1.81(2)	1.80(2)	1.85(3)	1.83(2)	1.81(2)	1.75(3)
U(4)-O(7)	1.83(2)	1.85(2)	1.84(2)	1.81(2)	1.82(2)	1.83(2)	1.81(2)	1.78(2)	1.82(2)	1.84(3)	1.82(2)	1.80(2)	1.75(3)
U(4)-O(13)	2.24(2)	2.23(2)	2.18(1)	2.25(2)	2.22(2)	2.23(2)	2.26(2)	2.24(2)	2.24(2)	2.21(2)	2.22(2)	2.24(2)	2.17(3)
U(4)-O(15)	2.32(2)	2.35(2)	2.41(2)	2.32(2)	2.34(2)	2.36(2)	2.28(2)	2.33(2)	2.37(2)	2.36(3)	2.37(3)	2.37(2)	2.47(3)
U(4)-O(14) <sub>b</sub>	2.33(2)	2.33(2)	2.35(1)	2.35(2)	2.34(2)	2.30(2)	2.30(2)	2.31(2)	2.31(1)	2.30(2)	2.32(2)	2.31(2)	2.40(3)
U(4)-O(12)	2.41(2)	2.40(2)	2.44(1)	2.42(2)	2.43(2)	2.42(2)	2.43(2)	2.41(2)	2.47(2)	2.46(3)	2.47(2)	2.43(2)	2.50(2)
U(4)-O(11) <sub>b</sub>	2.45(2)	2.45(2)	2.43(1)	2.45(2)	2.44(2)	2.44(2)	2.47(2)	2.45(2)	2.45(2)	2.46(2)	2.46(2)	2.45(1)	2.37(3)
<U(4)-O <sub>11</sub> >	1.82	1.84	1.84	1.82	1.82	1.83	1.84	1.80	1.81	1.85	1.83	1.81	1.75
<U(4)-φ>	2.35	2.35	2.36	2.36	2.35	2.35	2.35	2.35	2.37	2.36	2.37	2.36	2.38
Pb(1)-O(3) <sub>d</sub>	2.51(2)	2.50(2)	2.54(1)	2.54(2)	2.52(2)	2.52(2)	2.53(1)	2.48(2)	2.53(2)	2.53(2)	2.56(2)	2.54(2)	2.45(3)
Pb(1)-O(3)	2.51(2)	2.50(2)	2.54(1)	2.54(2)	2.52(2)	2.52(2)	2.53(1)	2.48(2)	2.53(2)	2.53(2)	2.56(2)	2.54(2)	2.45(3)
Pb(1)-O(7)	2.67(2)	2.65(2)	2.64(2)	2.68(2)	2.68(2)	2.67(2)	2.70(2)	2.72(2)	2.71(2)	2.67(2)	2.71(2)	2.70(2)	2.68(3)
Pb(1)-O(7) <sub>d</sub>	2.67(2)	2.65(2)	2.64(2)	2.68(2)	2.68(2)	2.67(2)	2.70(2)	2.72(2)	2.71(2)	2.67(2)	2.71(2)	2.70(2)	2.68(3)
Pb(1)-O(16)	2.71(3)	2.73(3)	2.85(2)	2.72(3)	2.78(4)	2.83(5)	2.74(3)	2.88(5)	2.86(2)	2.73(4)	2.79(4)	2.88(2)	3.17(7)
Pb(1)-O(17)	2.80(2)	2.84(3)	2.84(2)	2.78(3)	2.85(3)	2.84(3)	2.81(3)	2.79(3)	2.84(2)	2.78(3)	2.80(4)	2.85(2)	2.37(6)
Pb(1)-O(18)	2.87(3)	2.82(3)	2.76(3)	2.85(4)	2.83(3)	2.80(5)	2.82(3)	2.87(4)	2.85(3)	2.85(6)	2.83(5)	2.85(3)	2.53(8)
<Pb(1)-φ>	2.68	2.68	2.69	2.68	2.69	2.69	2.68	2.71	2.72	2.68	2.71	2.72	2.62
Pb(2)-O(2) <sub>e</sub>	2.53(2)	2.56(2)	2.56(1)	2.55(2)	2.56(2)	2.56(2)	2.57(2)	2.59(2)	2.55(2)	2.56(2)	2.57(2)	2.55(2)	2.84(3)
Pb(2)-O(2) <sub>f</sub>	2.53(2)	2.56(2)	2.56(1)	2.55(2)	2.56(2)	2.56(2)	2.57(2)	2.59(2)	2.55(2)	2.56(2)	2.57(2)	2.55(2)	2.84(3)
Pb(2)-O(17)	2.59(2)	2.56(2)	2.53(2)	2.61(3)	2.53(3)	2.53(3)	2.63(3)	2.60(3)	2.55(2)	2.57(3)	2.59(4)	2.54(2)	2.86(5)
Pb(2)-O(19)	2.62(2)	2.75(5)	2.85(3)	2.84(5)	2.81(5)	2.79(4)	2.76(4)	2.73(6)	2.82(4)	2.79(5)	2.87(7)	2.82(3)	
Pb(2)-O(8) <sub>f</sub>	2.69(2)	2.70(2)	2.73(1)	2.67(2)	2.71(2)	2.72(3)	2.65(2)	2.70(2)	2.70(2)	2.69(3)	2.69(2)	2.71(2)	3.16(3)
Pb(2)-O(8) <sub>e</sub>	2.69(2)	2.70(2)	2.73(1)	2.67(2)	2.71(2)	2.72(3)	2.65(2)	2.70(2)	2.70(2)	2.69(3)	2.69(2)	2.71(2)	3.16(3)
Pb(2)-O(6) <sub>f</sub>	2.92(2)	2.90(2)	2.88(1)	2.94(2)	2.89(2)	2.89(2)	2.95(2)	2.94(2)	2.90(2)	2.89(2)	2.88(2)	2.89(2)	2.70(3)
Pb(2)-O(6) <sub>e</sub>	2.92(2)	2.90(2)	2.88(1)	2.94(2)	2.89(2)	2.89(2)	2.95(2)	2.94(2)	2.90(2)	2.89(2)	2.88(2)	2.89(2)	2.70(3)
Pb(2)-O(16)	2.98(3)	2.90(4)	2.93(2)	2.96(3)	2.88(3)	2.86(4)	2.90(3)	2.76(4)	2.89(3)	3.01(5)	2.83(4)	2.91(3)	2.74(5)
Pb(2)-O(21) <sub>g</sub>													2.77(4)
<Pb(2)-φ>	2.72	2.73	2.74	2.75	2.73	2.72	2.74	2.73	2.73	2.74	2.73	2.73	2.83

a = -x, y + 1/2, z; b = -x + 1/2, y, -z + 1/2; c = -x + 1/2, y, 1/2, -z + 1/2; d = x, y, -z; e = -x + 1/2, y + 1/2, -z + 1/2; f = -x + 1/2, y + 1/2, z - 1/2; g = 1 - x, y + 1/2, z.

### Variation of Pb content and unit-cell parameters

The structural studies of 13 crystals of fourmarierite demonstrate significant variations in the Pb content, with total Pb ranging from 0.86 to 1.02 *apfu* (atoms per formula unit) for the natural crystals, and being 0.50 *apfu* for the synthetic crystal (Table 3). The Pb(1) site contains from ~70 to 100% Pb in the natural crystals,

but only 13% Pb in the synthetic crystal. The Pb(2) site is close to fully occupied in the natural crystals, and contains 87% Pb in the synthetic crystal.

The variation of the unit-cell parameters as a function of Pb content is shown in Figure 5. The unit-cell volume (Fig. 5d) decreases with increasing Pb content, presumably because of increased bond-strengths between the structural sheets and Pb in the interlayer.

TABLE 6. CHEMICAL COMPOSITIONS (WL. %) OF ELEVEN FOURMARIERITE CRYSTALS BY EMPA

	CMNMC81096				CMNMC81097				UMN753				UMN486	
	1	2	3	4	1	2	3	4	1	2	3	4	1	2
UO <sub>3</sub>	77.59	79.132	78.48	79.81	79.94	78.72	79.27	79.45	78.03	78.03	78.15	77.88	81.36	81.14
PbO	14.44	14.46	14.00	14.35	13.61	13.83	13.87	14.47	13.59	12.94	13.70	13.95	12.04	11.83
H <sub>2</sub> O	4.87	4.96	4.91	5.00	4.99	4.92	4.95	4.98	4.87	4.86	4.88	4.87	5.03	5.01
Total	96.90	98.55	97.39	99.16	98.54	97.47	98.09	98.90	96.49	95.83	96.73	96.70	98.43	97.98
*U <sup>6+</sup>			4.02				4.03				4.03			4.08
*Pb <sup>2+</sup>			0.94				0.91				0.90			0.77

	CMNMC81100			CMNMC81101			M30767			CMNMC81103				
	1	2	3	1	2	3	1	2	3	1	2	3	4	5
UO <sub>3</sub>	79.14	78.96	78.82	80.48	81.76	81.15	77.90	78.97	77.65	80.23	80.19	80.28	79.25	79.30
PbO	13.28	13.28	12.97	12.46	12.22	11.46	13.64	13.91	13.51	11.74	11.63	11.58	11.89	11.77
H <sub>2</sub> O	4.93	4.92	4.90	4.99	5.06	5.00	4.87	4.94	4.85	4.96	4.95	4.95	4.90	4.90
Total	97.35	97.16	96.69	97.93	99.04	97.61	96.41	97.82	96.01	97.08	96.77	96.81	96.04	95.97
U <sup>6+</sup>		4.05			4.08			4.03					4.08	
Pb <sup>2+</sup>		0.87			0.78			0.91					0.77	

	CMNMC53066				CMNMC81098			CMNMC81099				
	1	2	3	4	1	2	3	1	2	3	4	5
UO <sub>3</sub>	80.33	79.68	79.57	78.60	78.91	77.44	79.25	78.73	78.66	78.64	78.46	78.35
PbO	12.38	13.47	12.80	13.16	13.87	13.53	13.16	13.54	13.03	13.01	13.29	13.63
H <sub>2</sub> O	4.98	4.97	4.94	4.90	4.93	4.84	4.93	4.91	4.90	4.90	4.89	4.89
Total	97.69	98.12	97.31	96.66	97.71	95.81	97.34	97.18	96.59	96.55	96.64	96.87
U <sup>6+</sup>			4.05			4.04					4.04	
Pb <sup>2+</sup>			0.85			0.89					0.88	

\* Calculated based on 17 anions from the structure determination

The *a* dimension, which is parallel to the sheet of polyhedra, is relatively weakly affected by changes in the Pb content (Fig. 5a). Both the *b* and *c* dimensions show a large systematic decrease with increasing Pb (Figs. 5b, c). On the basis of the trends in Figure 5, the cell parameters given by Piret (1985) for fourmarierite are consistent with both Pb sites being close to 100% occupied by Pb, in agreement with his interpretation.

It is possible that a complete range of compositions between schoepite and fourmarierite occurs, although the fourmarierite crystals examined in the current study do not approach the full range. Such a series would have

to involve a phase transition from space group *Bb2<sub>1</sub>m* (fourmarierite) to *P2<sub>1</sub>ca* (schoepite). Linear regression of the unit-cell data for the natural crystals presented in Figure 5 indicates that the *b* and *c* parameters in the absence of Pb would be 16.86(8) and 14.67(4) Å (standard errors in brackets), which are similar to the values 16.813(5) and 14.731(4) Å obtained for schoepite by Finch *et al.* (1996). Inclusion of the data for the synthetic crystal results in intercepts of 16.86(3) and 14.99(4) Å for the *b* and *c* parameters, respectively, suggesting that a discontinuity occurs in the *c* parameter as a function of Pb content (Fig. 5c). An estimate of the Pb

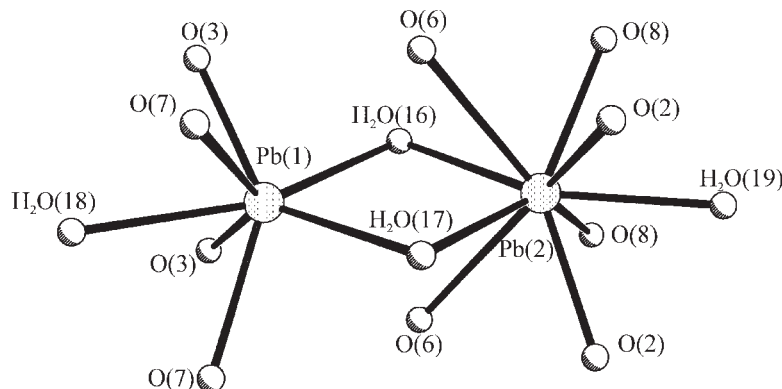


FIG. 1. The coordination polyhedra about the Pb(1) and Pb(2) sites in the natural crystals, which link to form a dimer of composition Pb<sub>2</sub>O<sub>14</sub>.

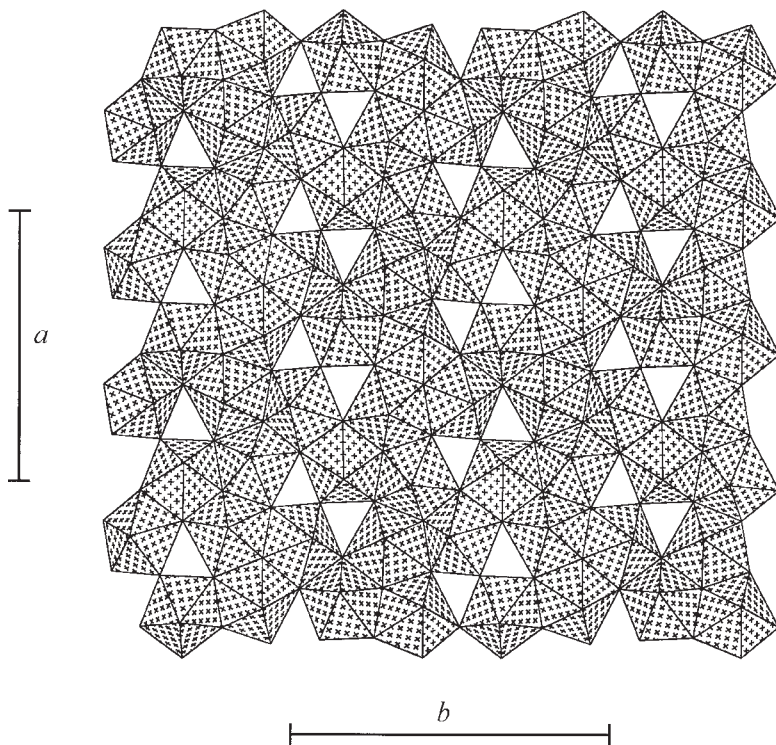


FIG. 2. Sheet of uranyl polyhedra in the structure of fourmarierite projected onto (001). The  $Ur\phi_5$  pentagonal bipyramids are shown shaded with crosses.

content of crystals of compositions intermediate between schoepite and fourmarierite may be obtained from the unit-cell parameters.

The total Pb contents of the natural crystals as derived by structure refinement and by analysis using an electron microprobe are compared in Figure 6. The microprobe analyses gave total Pb contents consistently ~8 mol.% lower than the structure refinements. The reason for this discrepancy is unknown, but may originate from factors such as crystal instability under the electron beam and the difficulty of identifying suitable standards for the analysis of these complex minerals.

#### Charge-balance mechanism

Variation of the Pb content of the interlayers of the structure of fourmarierite must be charge-balanced locally in the structure. Several possibilities exist to provide for the charge balance. Charged species other than  $Pb^{2+}$  in the interlayer could be involved, but careful inspection of difference-Fourier maps did not reveal additional sites in the interlayer, nor did the electron-microprobe analyses indicate constituents other than U and Pb. However, because of the dominance of U and Pb in the scattering of X-rays, small impurities of addi-

tional species in the interlayer cannot be ruled out. Another possibility is the substitution  $(OH)^- \rightarrow H_2O$  at any of the sites from O(16) to O(23) in the interlayer. On the basis of the bond-valences incident upon these  $H_2O$  sites, substitution of  $(OH)^-$  would lead to serious underbonding for the  $(OH)^-$  group, thus this charge-balancing mechanism seems unlikely.

The substitution  $(OH)^- \leftrightarrow O^{2-}$  within the sheet of uranyl polyhedra, at the equatorial vertices of the  $Ur\phi_5$  pentagonal bipyramids, could provide a local charge-balance mechanism. Such a substitution would be reflected by the bond-valence sums at the anion sites within the sheets; replacement of  $(OH)^-$  by  $O^{2-}$  should result in a shortening of the U–O bond lengths associated with the site. We examined the bond-valence sums at the anion sites for each crystal and found a relationship between the total Pb content of the crystal and the bond-valence sums at the O(12) and O(15) sites (Fig. 7), both of which are occupied mainly by  $(OH)^-$ . Note that neither of these sites is bonded to Pb, so that observed changes in the bond-valence sums may only be attributable to changes in U–O bond lengths. Other anion sites do not exhibit systematic changes in bond-valence sums with Pb content.



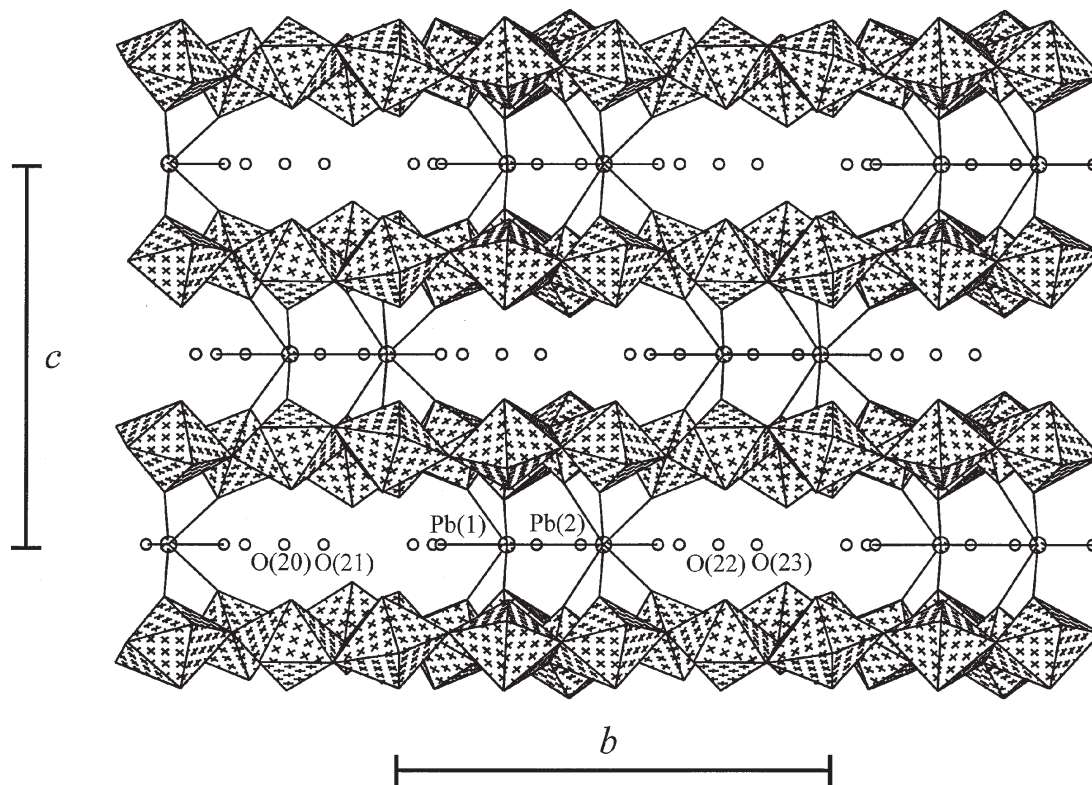


FIG. 3. The structure of fourmarierite projected onto (100). Large and small circles in the interlayer represent  $\text{Pb}^{2+}$  cations and  $\text{H}_2\text{O}$  groups, respectively.  $\text{Pb}-\phi$  bonds are shown by lines.

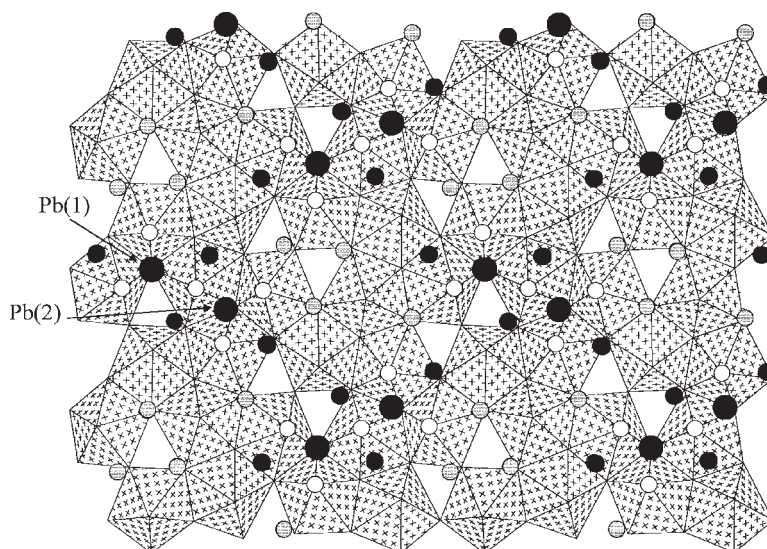


FIG. 4. Interlayer constituents projected onto the sheet of uranyl polyhedra at  $z \approx 0.25$ . Large solid black circles represent Pb cations at  $z \approx 0.5$ , small solid black circles represent  $\text{H}_2\text{O}$  groups bonded to Pb at  $z \approx 0.5$ , shaded circles represent H-bonded  $\text{H}_2\text{O}$  groups at  $z \approx 0.5$  in the interlayer, and open circles represent  $\text{O}_{\text{Ur}}$  bonded to Pb at  $z \approx 0.75$ .

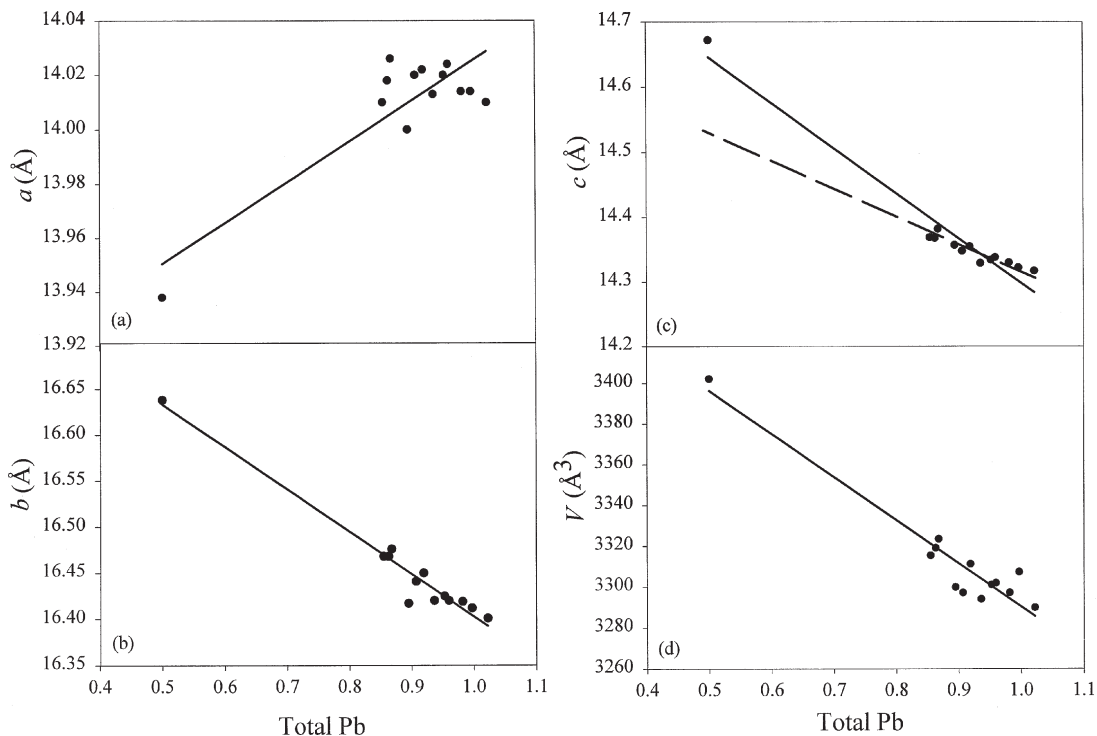


FIG. 5. Unit-cell parameters versus total Pb (*apfu*) obtained from crystal-structure refinement of thirteen single crystals of fourmarierite. The lines were obtained from linear regression of the data. In (c), the broken line was derived using data from the natural crystals only.

In the case of the O(15) site, the sum of bond valences [attributable to the U–O(15) bonds] ranges from 1.45 to 1.51 *vu* (valence units) in the natural crystals, and is 1.24 *vu* in the synthetic crystal. The sum

increases steadily with increasing Pb content in the crystal (Fig. 7b). This increase indicates that the U–O(15) bonds get stronger with increasing Pb content, consistent with an increase in the amount of  $O^{2-} \rightarrow (OH)^-$  substitution at the O(15) site. The situation is similar for the O(12) site (Fig. 7a). There, the bond-valence sums incident upon the anion increase from 1.34 in the synthetic crystal to ~1.65 in the natural crystals. These trends demonstrate that  $O^{2-} \leftrightarrow (OH)^-$  substitution within the sheets of uranyl polyhedra is the mechanism that provides charge balance as Pb varies in the interlayer.

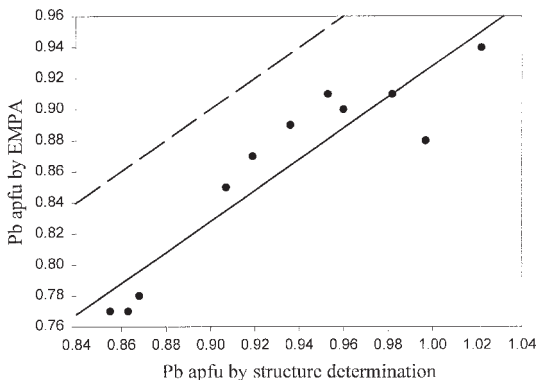


FIG. 6. Comparison of the proportion of Pb (*apfu*) determined by X-ray diffraction and electron-microprobe analysis. The broken line represents an ideal, iso-lead (*apfu*) segment from the two experimental methods.

#### Formula of fourmarierite

The structure determinations indicate that there are 32  $U^{6+}$  cations in the unit cell. Most O atoms can be designated as  $O^{2-}$ ,  $(OH)^-$  or  $H_2O$  groups on the basis of the bond-valence analysis (Table 7), except O(12) and O(15), which have bond-valence sums that range considerably in the crystals studied. The variability in these sums (Fig. 7) reflects the substitution of  $O^{2-} \leftrightarrow (OH)^-$  at these two sites. If *y* represents the total number of  $O^{2-}$  in sites O(12) and O(15), then there is  $(2-y)$   $(OH)^-$  in these sites. All  $O^{2-}$  and  $(OH)^-$  are located in the sheets of uranyl polyhedra, which therefore have the

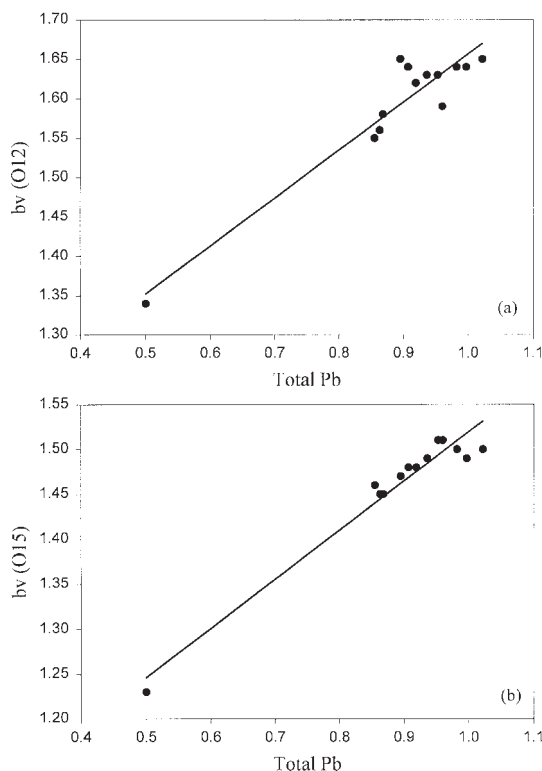


FIG. 7. Variation of bond-valence sums incident at selected anion sites as a function of Pb content. (a) The O(12) site. (b) The O(15) site. The lines were obtained by linear regression.

composition  $[(\text{UO}_2)_4\text{O}_{2+y}(\text{OH})_{5-y}]^{-(1+y)}$ . In order for the structure to be charge-balanced, there must be  $(1+y)$  Pb *apfu*. The formula of fourmarierite may be written as  $\text{Pb}_{1-x}[(\text{UO}_2)_4\text{O}_{3-2x}(\text{OH})_{4+2x}(\text{H}_2\text{O})_4]$ ,  $Z = 8$ . Where  $x = 0$ , this formula is identical to that given by Piret (1985). Where  $x = 1$ , the composition of the schoepite sheet results (Finch *et al.* 1996).

#### Interlayer of fourmarierite

For a given sheet-topology, the distribution of interlayer constituents is closely related to the type of interlayer species and the arrangement of the sheets of uranyl polyhedra on either side. The hydrogen-bond network in the interlayer of schoepite (Finch *et al.* 1996) may be considered to be interrupted by  $\text{Pb}^{2+}$  cations in the interlayer of fourmarierite, resulting in isolated Pb and  $\text{H}_2\text{O}$  clusters (Fig. 4). In the structure of fourmarierite, U sites of adjacent sheets are aligned, and if viewed perpendicular to the sheet, both of the Pb(1) and Pb(2) sites reside in triangular prisms defined by  $\text{O}_{Ur}$  atoms (Fig. 4). Similar configurations are observed for interlayer K cations between the  $\alpha\text{-U}_3\text{O}_8$ -type sheets in

TABLE 7. BOND-VALENCE\* (*vu*) ANALYSIS FOR A TYPICAL CRYSTAL OF FOURMARIERITE [CMNMC81098]

	U(1)	U(2)	U(3)	U(4)	Pb(1)	Pb(2)	$\Sigma^{\#}$
O(1)	1.61						1.61
O(2)	1.59					0.30×2↓	1.85
O(3)		1.59			0.32×2↓		1.73
O(4)		1.59					1.59
O(5)			1.61				1.61
O(6)			1.67			0.12×2↓	1.79
O(7)				1.53	0.24×2↓		1.60
O(8)				1.50		0.19×2↓	1.72
O(9)	0.42	0.38	0.50				1.30
O(10)	0.75	0.63	0.68				2.06
O(11)	0.48		0.30	0.47			1.25
O(12)	0.48	0.69		0.46			1.63
O(13)	0.67		0.60	0.77			2.04
O(14)		0.65		0.55			1.20
O(15)		0.41	0.59	0.49			1.49
O(16)					0.14	0.11	0.17
O(17)					0.14	0.33	0.39
O(18)					0.17		0.07
O(19)						0.14	0.14
O(20)							0
O(21)							0
O(22)							0
O(23)							0
$\Sigma$	6.00	5.94	5.95	5.77	1.57	1.80	

\*bond-valence parameters for  $\text{U}^{6+}$  from Burns *et al.* (1997a) and for Pb from Brese & O'Keeffe (1991).  $\#$  bond-valence contributions into the anion sums from Pb- $\phi$  bonds have been scaled by the corresponding occupancy of each Pb site.

the structure of compreignacite (Burns 1998b), for interlayer Pb between the  $\alpha\text{-U}_3\text{O}_8$ -type sheets in the structure of masuyite (Burns & Hanchar 1999), and for interlayer Ba between the  $\alpha\text{-U}_3\text{O}_8$ -type sheets in the structure of protasite (Pagoaga *et al.* 1987).

Because of the strong bonds within the uranyl ions, the  $\text{O}_{Ur}$  atoms receive  $\sim 1.7$  *vu* from the central  $\text{U}^{6+}$  cation. An important role of the interlayer constituents is to contribute valence to  $\text{O}_{Ur}$  atoms. There is a complementary relationship between the distribution of interlayer cations and hydrogen-bonded  $\text{H}_2\text{O}$  groups; hydrogen-bonded  $\text{H}_2\text{O}$  groups are usually present in the regions where there are no interlayer cations and provide hydrogen bonds to  $\text{O}_{Ur}$  atoms. Reduction of the amount of Pb in the Pb(1) and Pb(2) sites in fourmarierite impacts upon the sums of bond valences incident upon some of the  $\text{O}_{Ur}$  atoms, as these are bonded to  $\text{Pb}^{2+}$ . It is possible that partial replacement of  $\text{Pb}^{2+}$  by  $\text{H}_2\text{O}$  groups occurs, thus providing for hydrogen bonds that may be accepted by the  $\text{O}_{Ur}$  atoms.

#### DISCUSSION

The demonstration that  $(\text{OH})^- \leftrightarrow \text{O}^{2-}$  substitution within the sheets of uranyl polyhedra is the charge-balancing mechanism linked to Pb variation in the structure of fourmarierite is significant because this is the first demonstration of anion substitution within a sheet of uranyl polyhedra. This discovery has important structural implications because it permits a range of interlayer

contents without changing the topology of the sheet. These findings also indicate that there may be a link between the total charge on the fourmarierite sheet (and therefore the interlayer composition) and the pH of the solution that was in contact with the growing crystals. The Pb content of the interlayer, as well as the amount of hydrogen in the sheet of uranyl polyhedra, may prove to be a sensitive indicator of the geochemical conditions at the time of crystal growth.

The structure of fourmarierite may be obtained from that of schoepite by replacing selected  $(\text{OH})^-$  by  $\text{O}^{2-}$  in the sheet, insertion of Pb into the interlayer, and removal of specific  $\text{H}_2\text{O}$  groups. Foord *et al.* (1997) reported that mineral "A" may have the schoepite-type structure, but an appreciable amount of Pb was indicated by chemical analysis. Mineral "A" was originally described by Frondel (1956), and it probably formed as an alteration product in the early stages of corrosion of uraninite. Further studies are needed to determine whether mineral "A" may be Pb-bearing schoepite, Pb-poor fourmarierite such as the synthetic crystal obtained in the current study, or a distinct structure.

The finding that  $(\text{OH})^- \leftrightarrow \text{O}^{2-}$  substitution occurs in sheets of uranyl polyhedra based upon the fourmarierite anion-topology may be important for understanding the behavior of radionuclides during the alteration of nuclear waste. Buck *et al.* (1998) observed that dehydrated schoepite that had formed as an alteration product of spent fuel contains approximately 550 ppm Np, which is consistent with earlier predictions that uranyl phases can incorporate transuranic elements into their structures (Burns *et al.* 1997b). However, Np incorporated into dehydrated schoepite is most likely pentavalent, and a charge-balance mechanism is required for  $\text{Np}^{5+}$  to substitute for  $\text{U}^{6+}$ . In light of our findings, a possible charge-balance mechanism is  $(\text{OH})^- \leftrightarrow \text{O}^{2-}$  substitution in the sheets of uranyl polyhedra. We suggest that a considerable amount of Np could be incorporated into dehydrated schoepite without destabilizing the structure.

#### ACKNOWLEDGEMENTS

This research was supported by the National Science Foundation (EAR98-04723). We are grateful to the Canadian Museum of Nature, the Royal Ontario Museum and Prof. Rodney C. Ewing for providing the specimens used in this study. Mr. Robert Gault, Canadian Museum of Nature, provided electron-microprobe access and expertise. The manuscript was improved following detailed reviews by Drs. R.J. Finch and N. Blaton, and editorial work by Drs. R.F. Martin and J.M. Hughes.

#### REFERENCES

- ABDELOUAS, A., LUTZE, W. & NUTTALL, H.E. (1999): Uranium contamination in the subsurface: characterization and remediation. *Rev. Mineral.* **38**, 433-473.
- BRESE, N.E. & O'KEEFFE, M. (1991): Bond-valence parameters for solids. *Acta Crystallogr.* **B47**, 192-197.
- BUCK, E.C., FINCH, R.J., FINN, P.A. & BATES, J.K. (1998): Retention of Np in uranyl alteration phases formed during spent fuel corrosion. *Mater. Res. Soc., Symp. Proc.* **506**, 83-91.
- BURNS, P.C. (1997): A new uranyl oxide hydrate sheet in the structure of vandendriesscheite: implication for mineral paragenesis and the corrosion of spent nuclear fuel. *Am. Mineral.* **82**, 1176-1186.
- \_\_\_\_\_ (1998a): The structure of richetite, a rare lead uranyl oxide hydrate. *Can. Mineral.* **36**, 187-199.
- \_\_\_\_\_ (1998b): The structure of compreignacite,  $\text{K}_2[(\text{UO}_2)_3\text{O}_2(\text{OH})_3]_2(\text{H}_2\text{O})_7$ . *Can. Mineral.* **36**, 1061-1067.
- \_\_\_\_\_ (1998c): The structure of boltwoodite and implications of solid solution toward sodium boltwoodite. *Can. Mineral.* **36**, 1069-1075.
- \_\_\_\_\_ (1999): A new complex sheet of uranyl polyhedra in the structure of wölsendorffite. *Am. Mineral.* **84**, 1661-1673.
- \_\_\_\_\_ (2000a): A new uranyl silicate sheet in the structure of haiweeite and comparison to other uranyl silicates. *Can. Mineral.* **38** (in press).
- \_\_\_\_\_ (2000b): A new uranyl phosphate chain in the structure of parsonsite. *Am. Mineral.* **85**, 801-805.
- \_\_\_\_\_, EWING, R.C. & HAWTHORNE, F.C. (1997a): The crystal chemistry of hexavalent uranium: polyhedron geometries, bond-valence parameters, and polymerization of polyhedra. *Can. Mineral.* **35**, 1551-1570.
- \_\_\_\_\_, \_\_\_\_\_ & MILLER, M.L. (1997b): Incorporation mechanisms of actinide elements into the structures of  $\text{U}^{6+}$  phases formed during the oxidation of spent nuclear fuel. *J. Nucl. Mater.* **245**, 1-9.
- \_\_\_\_\_ & FINCH, R.J. (1999): Wyartite: crystallographic evidence for the first pentavalent-uranium mineral. *Am. Mineral.* **84**, 1456-1460.
- \_\_\_\_\_ & HANCHAR, J.M. (1999): The structure of masuyite,  $\text{Pb}[(\text{UO}_2)_3\text{O}_3(\text{OH})_2](\text{H}_2\text{O})_3$ , and its relationship to protasite. *Can. Mineral.* **37**, 1483-1491.

- \_\_\_\_\_ & HILL, F.C. (2000a): Implications of the synthesis and structure of the Sr analogue of curite. *Can. Mineral.* **38**, 175-182.
- \_\_\_\_\_ & \_\_\_\_\_ (2000b): A new uranyl sheet in  $K_5[(UO_2)_{10}O_8(OH)_9](H_2O)$ : implications for understanding sheet anion-topology. *Can. Mineral.* **38**, 163-174.
- \_\_\_\_\_, OLSON, R.A., FINCH, R.J. HANCHAR, J.M. & THIBAUT, Y. (2000):  $KNa_3(UO_2)_2(Si_4O_{10})_2(H_2O)_4$ , a new compound formed during vapor hydration of an actinide-bearing borosilicate waste glass. *J. Nucl. Mater.* **278**, 290-300.
- FINCH, R.J., COOPER, M.A., HAWTHORNE, F.C. & EWING, R.C. (1996): The crystal structure of schoepite,  $[(UO_2)_8O_2(OH)_{12}](H_2O)_{12}$ . *Can. Mineral.* **34**, 1071-1088.
- \_\_\_\_\_ & EWING, R.C. (1992): The corrosion of uraninite under oxidizing conditions. *J. Nucl. Mater.* **190**, 133-156.
- FINN, P.A., HOH, J.C., WOLF, S.F., SLATER, S.A. & BATES, J.K. (1996): The release of uranium, plutonium, cesium, strontium, technetium and iodine from spent fuel under unsaturated conditions. *Radiochim. Acta* **74**, 65-71.
- FOORD, E.E., KORZEB, S.L., LICHTÉ, F.E. & FITZPATRICK, J.J. (1997): Additional studies on mixed uranyl oxide-hydroxide hydrate alteration products of uraninite from the Palermo and Ruggles granitic pegmatites, Grafton Country, New Hampshire. *Can. Mineral.* **35**, 145-151.
- FRONDEL, C. (1956): Mineral composition of gummite. *Am. Mineral.* **41**, 539-568.
- \_\_\_\_\_ (1958): Systematic mineralogy of uranium and thorium. *U.S. Geol. Surv., Bull.* **1064**.
- HILL, F.C. & BURNS, P.C. (1999): The structure of a synthetic Cs uranyl oxide hydrate and its relationship to compreignacite. *Can. Mineral.* **37**, 1283-1288.
- LI, YAPING & BURNS, P.C. (2000a): Investigations of crystal-chemical variability in lead uranyl oxide hydrates. I. Curite. *Can. Mineral.* **38**, 729-737.
- \_\_\_\_\_ & \_\_\_\_\_ (2000b): Synthesis and crystal structure of a new Pb-uranyl oxide hydrate with a framework structure that contains channels. *Can. Mineral.* **38** (in press).
- PAGOAGA, M.K., APPLEMAN, D.E. & STEWART, J.M. (1987): Crystal structures and crystal chemistry of the uranyl oxide hydrates becquerelite, billicite, and protasite. *Am. Mineral.* **72**, 1230-1238.
- PIRET, P. (1985): Structure cristalline de la fourmariérite,  $Pb(UO_2)_4O_3(OH) \cdot 4H_2O$ . *Bull. Minéral.* **108**, 659-665.
- \_\_\_\_\_, DELIENS, M., PIRET-MEUNIER, J. & GERMAIN, G. (1983): La sayrite,  $Pb_2[(UO_2)_5O_6(OH)_2]_4 \cdot 4H_2O$ , nouveau minéral; propriétés et structure cristalline. *Bull. Minéral.* **106**, 299-304.
- TAYLOR, J.C., STUART, W.L. & MUMME, I.A. (1981): The crystal structure of curite. *J. Inorg. Nucl. Chem.* **43**, 2419-2423.
- WRONKIEWICZ, D.J., BATES, J.K., WOLF, S.F. & BUCK, E.C. (1996): Ten-year results from unsaturated drip tests with  $UO_2$  at 90°C: implications for the corrosion of spent nuclear fuel. *J. Nucl. Mater.* **238**, 78-95.

Received December 20, 1999, revised manuscript accepted May 3, 2000.



